

Fast Screening Algorithm for Rotation and Scale Invariant Template Matching

Bolin Liu
McMaster University
liub30@mcmaster.ca

Xiao Shu
McMaster University
shux@mcmaster.ca

Xiaolin Wu
Shanghai Jiao Tong University
xwu510@sjtu.edu.cn

Abstract

This paper presents a generic pre-processor for expediting conventional template matching techniques. Instead of locating the best matched patch in the reference image to a query template via exhaustive search, the proposed algorithm rules out regions with no possible matches with minimum computational efforts. While working on simple patch features, such as mean, variance and gradient, the fast pre-screening is highly discriminative. Its computational efficiency is gained by using a novel octagonal-star-shaped template and the inclusion-exclusion principle to extract and compare patch features. Moreover, it can handle arbitrary rotation and scaling of reference images effectively. Extensive experiments demonstrate that the proposed algorithm greatly reduces the search space while never missing the best match.

1 Introduction

Template matching, a fundamental operation in computer vision, is to locate the best matched patch in a reference image to a given query template. While finding an object in image seems to be trivial for human in general, it is a surprisingly challenging problem for computer algorithms. Most existing template matching techniques are very time-consuming and demand a lot of computational resources to obtain relatively reliable results in real-world applications, where geometric distortions between the reference image and query template are unavoidable.

To handle geometric distortions like a simple change in scale or orientation, conventional patch based template matching techniques, which compare the template directly with all the candidate patches in succession, have to rely on an exhaustive search of all the combinations of different scales and rotations. In comparison, newly emerged feature based techniques are more efficient and robust for matching a template with deformations. The basic idea of feature based template matching is to extract some statistical features from the query template and check if these features also occur in some patches in the reference image. As matched features do not need to appear at the exact matched

positions, feature based techniques are more resilient to geometric distortions as long as both of the reference image and query template have distinctive features. However, with regard to overall matching speed, feature based techniques are still unsatisfactory; they commonly require a computationally intensive process to generate features for different scales, and the whole matching process can be slow for high-resolution images.

In this paper, we propose a scale and rotation invariant template matching pre-processor for expediting conventional patch and feature based template matching techniques. Instead of pinpointing the best matched patch, this pre-processor rapidly rules out regions of no possible matches using simple patch features, such as mean, variance and gradient. After the pre-processing procedure, the remainder parts of the reference image are passed to a more accurate but slower template matching technique to locate the exact position of the best match. As the regions to search are greatly reduced in the pre-processing step, the accurate template matching technique needs to process far fewer pixels or patches hence it runs much faster than having to process the whole image.

To make this two-stage method a viable strategy, the cost of the pre-processing, i.e., the time spent on identifying no match regions, must be less than the time saved in the later accurate template matching stage. Thus, the major challenge in the design of the pre-processing algorithm is to make its computational complexity extremely low while effective enough to mark as many unmatched regions as possible. On the other hand, since the accurate template matching technique in the second stage only operates on the unmarked regions from the first stage, if the best matched patch has already been incorrectly marked as unmatched, the two-stage method would fail to locate the best match. Therefore, in order to avoid affecting the success rate of the subsequent template matching, the false positive rate of the pre-processing algorithm must be made very low.

The remainder of this paper is organized as follows. Section 2 reviews some of the related template matching techniques. Section 3 discusses the patch features employed by the proposed technique. Sections 4 and 5 elaborate on how to make the proposed technique rotation and scale invariant, respectively. Section 6 presents experimental results

and Section 7 concludes.

2 Related Work

A great amount of research effort has been dedicated to designing efficient and effective template matching techniques. Based on conventional full search matching, Alkhansari proposed a technique that reduces search space by pruning unmatched regions using a downsampled reference image [7]. Pele and Werman developed a method to determine the optimal step size of sliding windows for full search matching [20]. On the topic of latest full search equivalent techniques, Ouyang *et al.* provided a comprehensive survey and compared the performances of several popular methods [19].

Template matching techniques based on SSD or normalized cross correlation (NCC) can be accelerated using frequency domain approaches [1] or summer area tables [12, 3, 25]. SAD, SSD and NCC based techniques are often highly efficient in terms of computational cost, however, they are not flexible enough to handle geometric transformation between the reference image and query template efficiently. Ullah and Kaneko used the orientation code to represent gradient information in a patch for approximating rotation angles as well as for rotation invariant matching [24]. Choi and Kim proposed to combine circular projection and Zernike moments to achieve rotation invariance [2]. Their method was later improved by Kim [10]. Based on circular projection, Kim used the Fourier coefficients of radial projections as rotation invariant features. Lin and Chen used ring projection transform to establish parametric template vector for differently scaled template to get invariance for rotation and scale [14]. Moreover, Tsai and Chiang [23] solved the rotation problem using wavelet decompositions and ring projection. Korman *et al.* [11] approximated the 2D affine transformation in reference image by constructing a transformation net with SAD error level δ . Wakahara and Yamashita [26] proposed a global projection transform correlation method to deal with arbitrary 2D transformation.

Recently, feature-based image matching methods, such as scale invariant feature transform (SIFT) [15], become more popular. After obtaining rotation and scale invariant features for both template and reference image, data fitting algorithm like RANSAC [6] are used for finding matching patterns. ASIFT extends SIFT to be fully affine invariant [18]. Dekel *et al* introduced a novel similarity measure termed best-buddies similarity (BBS) for comparing the features of two patches [4]. BBS is robust against many types of geometric deformations and well suited for video tracking applications. These feature-based methods are generally time consuming due to their heavy processes for generating feature descriptors, also they may fail to work if the template is relatively small or lightly textured.

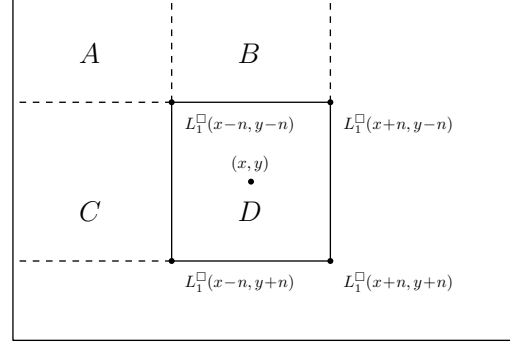


Figure 1: The sum $S_1^\square(x, y)$ of area D is a simple linear combination of $L_1^\square(x+n, y+n)$, $L_1^\square(x-n, y+n)$, $L_1^\square(x+n, y-n)$, $L_1^\square(x-n, y-n)$, which represent the sums of area $A + B + C + D$, $A + C$, $A + B$ and A , respectively

3 Patch Features

The proposed algorithm rules out regions with no possible matches based on whether or not the patches in these regions share the same features with the given query template. Patch features employed by conventional template matching techniques are often complex and computationally expensive due to the accuracy and robustness requirements for pinpointing the best match. However, since the proposed pre-processing algorithm only needs to rule out patches that are significantly different from the query template, simple patch features, such as mean, variance and gradient, are sufficient for distinguishing a majority of those unmatched patches.

The mean of a patch, the inner product of the patch with a box average kernel, can be calculated efficiently by using the inclusion-exclusion principle. As presented in [3], it only needs one addition and two subtractions to calculate the sum of the pixel intensity of an arbitrary rectangular area using a summed area table, which is also known as integral image. The idea is that, if we know the sum $L_1^\square(x, y)$ of a rectangular area with top-left corner $(1, 1)$ and bottom-right corner (x, y) for any given pixel (x, y) of image I , as shown in Figure 1, then we can calculate the sum $S_1^\square(x, y)$ of any $2n \times 2n$ patch centered at (x, y) as follows,

$$\begin{aligned} S_1^\square(x, y) &= \sum_{i=x-n+1}^{x+n} \sum_{j=y-n+1}^{y+n} I(i, j) \\ &= L_1^\square(x+n, y+n) - L_1^\square(x-n, y+n) \\ &\quad - L_1^\square(x+n, y-n) + L_1^\square(x-n, y-n), \end{aligned} \quad (1)$$

where the summed area table $L_1^\square(x, y)$, by its definition, is,

$$L_1^\square(x, y) = \sum_{i=1}^x \sum_{j=1}^y I(i, j). \quad (2)$$

Given the sum of a patch centered at (x, y) , the mean

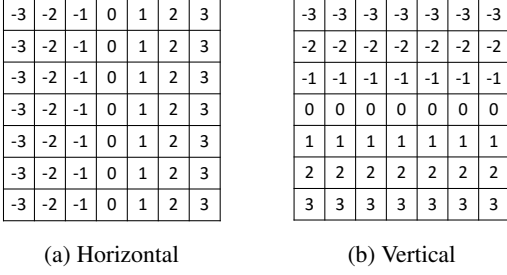


Figure 2: The extended 7×7 Prewitt kernels, which are basically linear gradient ramps.

$S_\mu^\square(x, y)$ of the patch is,

$$S_\mu^\square(x, y) = S_1^\square(x, y)/(2n)^2. \quad (3)$$

The summed area table $L_1^\square(x, y)$ for image I can be constructed efficiently by using a pass of horizontal cumulative sum on every row of I followed by a pass of vertical cumulative sum on every column. Since the cumulative sums of different rows (or columns) are independent, it is easy to accelerate the construction process with parallel computing architecture, such as GPU, by calculating the cumulative sums of rows (or columns) concurrently. After the linear-time construction of the summer area table $L_1^\square(x, y)$, each of the following query for the intensity sum $S_1^\square(x, y)$ or mean $S_\mu^\square(x, y)$ of an arbitrary patch only requires constant time regardless of the size the patch.

In addition to the mean of a patch, the proposed algorithm also employs two other linear features, the horizontal and vertical gradients. The horizontal and vertical gradient of a patch, representing the rate of pixel intensity change of the patch from left to right and from top to bottom respectively, are the inner products of the patch with the extended Prewitt kernels [9] of the same size. The extended Prewitt kernels are basically linear gradient ramps as shown in Figure 2, and they are defined as follows,

$$\begin{aligned} P_x(x, y) &= x - \frac{m+1}{2}, \\ P_y(x, y) &= y - \frac{m+1}{2}, \end{aligned} \quad (4)$$

Choosing horizontal and vertical gradients as patch features is based on the fact that the first three principle components of natural image patches in principle component analysis (PCA) are the box average kernel, vertical extended Prewitt kernel and horizontal extended Prewitt kernel, respectively (as shown in Figure 3). Thus, for distinguishing patches, these kernels have the strongest discriminating power among all the combinations of any three linear features.

In a similar fashion as the sum of a patch as in Eq. 1, gradient of a patch can also be calculated efficiently by using the inclusion-exclusion principle. For instance, the horizontal gradient $S_x^\square(x, y)$ of a $2n \times 2n$ patch centered at (x, y)

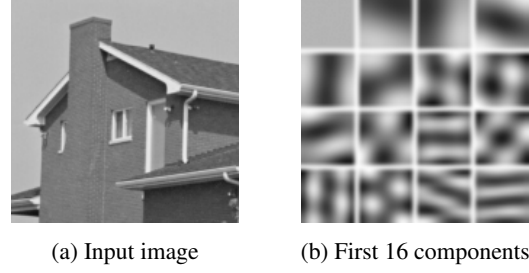


Figure 3: A sample image and the first 16 principle components of all the 16×16 patches in the image [5].

is,

$$\begin{aligned} S_x^\square(x, y) &= \sum_{i=x-n+1}^{x+n} \sum_{j=y-n+1}^{y+n} (i-x) \cdot I(i, j) \\ &= L_x^\square(x+n, y+n) - L_x^\square(x-n, y+n) \\ &\quad - L_x^\square(x+n, y-n) + L_x^\square(x-n, y-n) \\ &\quad - xS_1^\square(x, y) \end{aligned} \quad (5)$$

where $L_x^\square(x, y)$, the summed area map of image $i \cdot I(i, j)$, is,

$$L_x^\square(x, y) = \sum_{i=1}^x \sum_{j=1}^y i \cdot I(i, j). \quad (6)$$

Similarly, the vertical gradient $S_y^\square(x, y)$ of the patch is tractable with the same technique.

Another patch feature employed by the proposed algorithm is variance. Given the mean $S_\mu^\square(x, y)$ and second moment $S_2^\square(x, y)$ of a $2n \times 2n$ patch, the variance $S_\sigma^\square(x, y)$ of the patch can be obtained as,

$$S_\sigma^\square(x, y) = S_2^\square(x, y)/(2n)^2 - [S_\mu^\square(x, y)]^2. \quad (7)$$

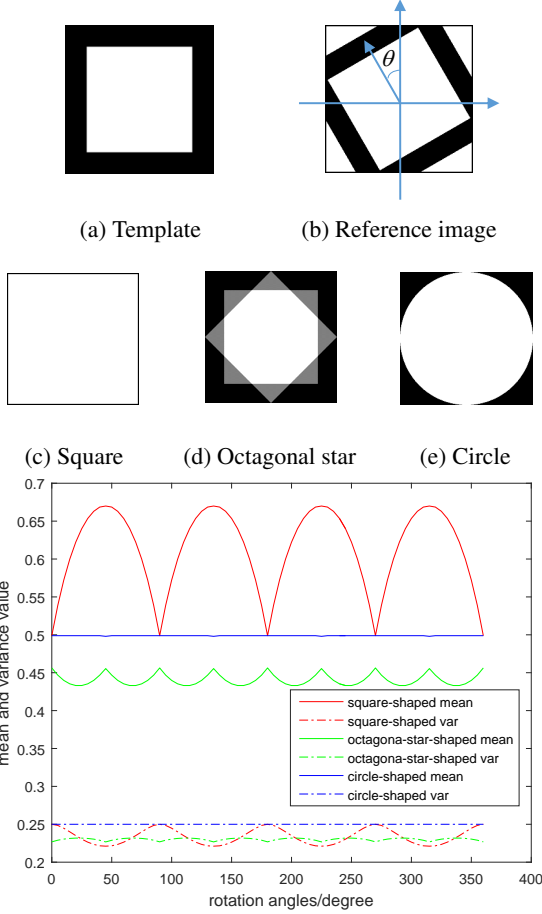
Since the second moment $S_2^\square(x, y)$ of each patch,

$$S_2^\square(x, y) = \sum_{i=x-n+1}^{x+n} \sum_{j=y-n+1}^{y+n} [I(i, j)]^2, \quad (8)$$

only requires constant time to calculate with the summed area table of $[I(i, j)]^2$, we can acquire the variance of an arbitrary patch efficiently as well.

4 Rotation Invariance

The patch features discussed in the previous section are excellent indicators for ruling out unmatched patches if the object in the query template and reference image shares the same orientation and scale. However, if that is not the case, a small mismatch between the orientations of the query template and reference image could result distinct patch features for the same object, causing mistakes in matching



(f) The mean and variance of a patch plotted as a function of image rotation angle.

Figure 4: Octagonal-star-shaped template is much more robust against rotation than square template.

the object. This over-sensitivity to orientation is due to two problems: first, some of patch features like horizontal and vertical gradients are not rotation invariant; second, the shape of the template is also not rotation invariant.

The first problem can be easily resolved by replacing the horizontal and vertical gradients with the magnitude of gradient,

$$S_m^\square(x, y) = \sqrt{[S_x^\square(x, y)]^2 + [S_y^\square(x, y)]^2}, \quad (9)$$

which is robust against rotation and still simple to calculate.

To solve the second problem, we need to change the shape of the template. Commonly, the query template is a square image patch provided by the user. Given the template, the pre-processing algorithm then examines the features of every square patch of the same size as the template in the reference image. The drawback of using square patch is the area covered by a square patch are variant to image rotation. For instance, the reference image shown in Figure 4 is a black framed box on white background. A rotation of

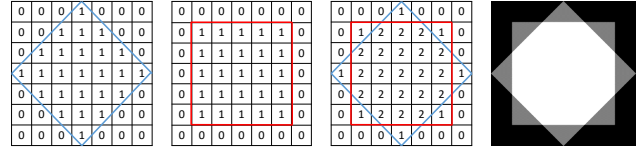


Figure 5: An example of octagonal-star-shaped 7×7 template (the third figure), which is the superposition of a square (the second figure) and a diamond (the first figure).

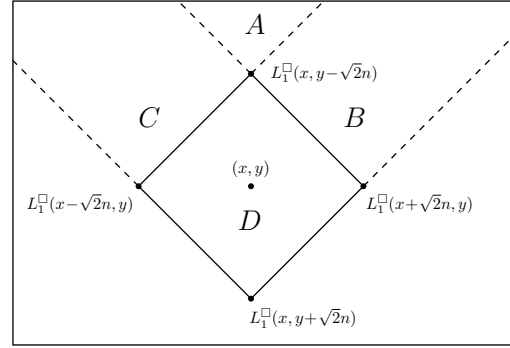


Figure 6: The sum $S_1^\diamond(x, y)$ of area D is a simple linear combination of $L_1^\diamond(x, y + \sqrt{2}n)$, $L_1^\diamond(x - \sqrt{2}n, y)$, $L_1^\diamond(x + \sqrt{2}n, y)$, $L_1^\diamond(x, y - \sqrt{2}n)$, which represent the sums of area $A + B + C + D$, $A + C$, $A + B$ and A , respectively

the reference image moves some of the white background pixels into the window centered at the box while cropping out some of the black frame pixels. The resulting change in the set of pixels in the window alters all its patch features such as the mean and variance as in Figure 4.

Ideally, the best template shape for rotation invariant matching is a circle, but it is not possible to accelerate the feature calculation of an arbitrary circular patch using the inclusion-exclusion technique introduced previously. Thus, we propose octagonal-star-shaped template, which approximates to a circle but still has efficient feature calculation algorithm. An octagonal star is the superposition of a square and a diamond (square rotated by 45°) of the same size as depicted in Figure 5. The weighted mean $S_\mu(x, y)$ of an octagonal-star-shaped template, for example, is the arithmetic average of the mean $S_\mu^\square(x, y)$ of the square and the mean $S_\mu^\diamond(x, y)$ of the diamond in the template, i.e.,

$$S_\mu(x, y) = \frac{1}{2}[S_\mu^\square(x, y) + S_\mu^\diamond(x, y)], \quad (10)$$

Similar to the previous rectangular case, if the sum $L_1^\diamond(x, y)$ of the triangular area with right angle vertex (x, y) , as shown in Figure 6, is known for any x, y , where $L_1^\diamond(x, y)$ is,

$$L_1^\diamond(x, y) = \sum_{i=\max(y-x, 1)}^{\min(y+x, M)} \sum_{j=1}^{y-|x-i|} I(i, j) \quad (11)$$

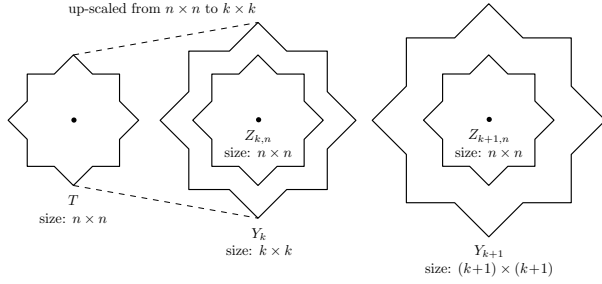


Figure 7: Templates in different scales.

and M is the width of the image. Then, by the inclusion-exclusion principle, we can calculate the sum $S_1^\diamond(x, y)$ and mean $S_\mu^\diamond(x, y)$ of a $2n \times 2n$ diamond area centered at (x, y) using one addition and two subtractions as follows [13, 16],

$$S_1^\diamond(x, y) = L_1^\diamond(x, y + \sqrt{2}n) - L_1^\diamond(x - \sqrt{2}n, y) - L_1^\diamond(x + \sqrt{2}n, y) + L_1^\diamond(x, y - \sqrt{2}n) \quad (12)$$

$$S_\mu^\diamond(x, y) = S_1^\diamond(x, y) / (2n)^2 \quad (13)$$

Same as $L_1^\square(x, y)$, the construction of the summed triangular area map $L_1^\diamond(x, y)$ is tractable in linear time using two diagonal passes of cumulative sum. Besides the mean, other patch features, such as the variance and magnitude of gradient, of a octagonal-star-shaped template can also be computed efficiently by combining the features of the square and diamond areas in the template.

5 Scale Invariance

Another challenge for the proposed pre-processing algorithm is how to handle the scale difference between the query template and reference image. In the previous sections, we assume that the scales of the query template and reference image are identical, hence the best matched patch must be of the exact same size as the query template. However, this assumption is impractical in most real-world applications; the scale information is usually unknown and the best matched patch may be larger or smaller than the query template.

One solution to this scale invariant problem is simply to scale the query octagonal-star shaped template to difference sizes and then check if some of the resized templates has a well matched patch of the same size in the reference image [8]. If the best matched patch can be any size from $\alpha n \times \alpha n$ to $\beta n \times \beta n$, where n is the side length of the query template and α, β are some constants, then there are $\beta n - \alpha n = O(n)$ different possible template scales to examine. In the case of our pre-processing algorithm, as comparing the features of a template to all patches of the same size requires $O(M^2 + n^2)$ time for a $M \times M$ reference image, the overall time complexity for scale invariant screening with the aforementioned method is $O(M^2 n + n^3)$.

The exhaustive search strategy is inefficient and unsuited for our goal of fast screening of unmatched regions, especially when the query template is large. But this method can be greatly accelerated if we only check patches of a few different sizes in the reference image instead of enumerating every possible sizes. The idea is based on an assumption that, if two patches of the same size have matched central area, then these two patches might also match. For instance, given an $n \times n$ query template T , suppose that image Y_k of size $k \times k$ is an up-scaled version of T as shown in Figure 7, and the patch feature vector $f_{k,n}$ of the $n \times n$ center of Y_k , namely $Z_{k,n}$, matches a patch P_n in the reference image, then the $k \times k$ patch P_k centered at the same location as P_n might also match the features of Y_k . Similarly, given Y_{k+1} , a $(k+1) \times (k+1)$ version of T , if it matches a patch P_{k+1} of the same size, their $n \times n$ central areas, $Z_{k+1,n}$ and P_n , should have matching features. Therefore, to find the matched patches of either size $k \times k$ or $(k+1) \times (k+1)$, we only have to look through all the $n \times n$ patches in the reference image; there is no need for calculating the features for patches of different sizes.

The assumption that matched central areas indicate matched patches is not always true obviously, however, it only slightly increases the possibility of mistaking a wrong patch as matched, as long as the examined center area is sufficiently large, i.e., n is not much smaller than k . Moreover, the best match should have a matched central area to the query template hence not affected by the assumption. Therefore, despite the limitation of the assumption, the pre-processor can still rule out a great amount of unlikely matched areas without removing the best match for the next stage template matching algorithm.

Although this method can process the templates of several different scales with only the patches of one fixed size, it still needs to compare the features of a patch with the features of the query template of every scale. Thus, the time complexity for comparing all the templates with all the patches is still $O(M^2 n)$. To make the feature comparison function more efficient, we can aggregate the features of the templates of different scales together into a feature set F_n ,

$$F_n = \{f_{k,n} \mid n \leq k \leq \lambda n\}, \quad (14)$$

which includes all the feature vectors of the scaled templates of size from $n \times n$ to $\lambda n \times \lambda n$. Now given F_n , we can examine if a $n \times n$ patch P matches $Z_{k,n}$ for some $k \in [n, \lambda n]$ by testing the membership of the feature vector of P in set F_n . If the size of the best matched patch ranges from $\alpha n \times \alpha n$ to $\beta n \times \beta n$, then we need to repeat the process $\log_\lambda(\beta/\alpha)$ times for different scale ranges.

The feature set F_n can be implemented using a membership array \hat{F}_n with $\hat{F}_n(Q(f)) = 1$ for any $f \in F_n$, where $Q(f)$ is a quantizer for feature vector. For simplicity's sake, assume that there is only one feature to consider and $Q(f) = \lfloor f/q + \frac{1}{2} \rfloor$ is a uniform quantizer with quantization factor q . For some $f \in F_n$, if both $Q(f - q/2)$ and

$Q(f+q/2)$ are marked as 1 in \hat{F}_n in addition to $Q(f)$, then, given a feature g , $\hat{F}_n(Q(g)) = 1$ as long as $|f - g| < q/2$. Thus, quantization factor q is a parameter that sets how similar the features of two patches should be before counting them as matched.

Algorithm 1: Screening pre-processor for scale invariant template matching

Data: I , reference image
Data: T , query template
Data: $[\alpha, \beta]$, scale range
Result: R , set of possible matched patches

```

1 begin
2    $\lambda \leftarrow \sqrt{2}$ 
3    $n \leftarrow \text{get\_width}(T)$ 
4    $R \leftarrow \emptyset$ 
5    $m \leftarrow \beta n$ 
6   while  $m \geq \alpha n$  do
7      $m \leftarrow m/\lambda$ 
8      $F_m \leftarrow \emptyset$ 
9     for  $k \leftarrow m$  to  $m\lambda$  do
10       $Y_k \leftarrow \text{scale}(T, k \times k)$ 
11       $Z_{k,m} \leftarrow \text{crop\_center}(Y_k, m \times m)$ 
12       $f_{k,m} \leftarrow Q(\text{features}(Z_{k,m}))$ 
13       $F_m \leftarrow F_m \cup \{f_{k,m}\}$ 
14     foreach  $m \times m$  patch  $P$  in  $I$  do
15       if  $Q(\text{features}(P)) \in F_m$  then
16          $R = R \cup \{P\}$ 

```

This efficient scale invariant pre-processing algorithm is summarized in Algorithm 1. Since a membership array only requires constant time to initialize and constant time to access one element regardless of the size of the array [21], the time complexity for constructing F_n is $O(n^3)$ and the time complexity for testing the features of all the patches is $O(M^2)$. Overall, the proposed scale invariant pre-processing algorithm requires $O(M^2 + n^3)$ time. Considering that the reference image is generally much larger than the query template, the increase in the asymptotic computational complexity from $O(M^2 + n^2)$ due to the addition of scale invariant support is insignificant.

Patch features of different scales calculated for scale invariant matching benefit the accuracy of matching as well. As discussed previously, we consider a $k \times k$ patch P_k matches template Y_k of size $k \times k$ if their $n \times n$ central areas P_n and $Z_{k,n}$ share the similar features. In addition to P_n and $Z_{k,n}$, if the smaller $(n/\lambda) \times (n/\lambda)$ central areas $P_{n/\lambda}$ and $Z_{k,n/\lambda}$ also have matched features, patch P_k is even more likely to be a match to the query template. Therefore, given a query template, the feature comparison process should not be limited only to the large central area; the additional features from smaller center areas, as illustrated in Figure 8a, can be used to provide extra details

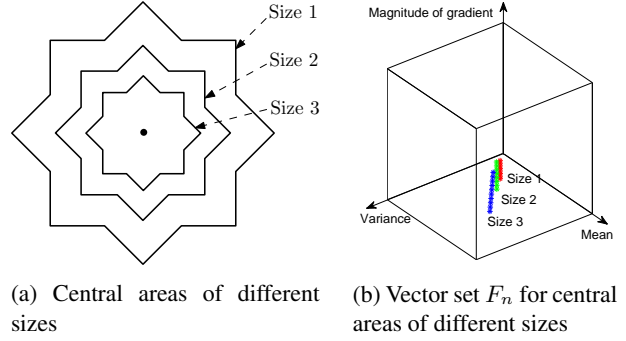


Figure 8: Features from different central areas of a patch are utilized together to improve matching accuracy.

about a patch, making the matching process more accurate and reliable. Figure 8b plots scale invariant feature vector set F_n for each central area of a query template. In our scale invariant algorithm, if any one of three central areas of a patch does not match the features of the corresponding areas of the template, the patch is marked as unmatched. Since these features of different scales ($n, n/\lambda, n/\lambda^2, \dots$) have already been calculated for scale invariant matching, the extra cost for utilizing these features is negligible.

6 Experimental Results

To evaluate the performance of the proposed technique, we implement the rotation and scale invariant pre-processing algorithm, as shown in Algorithm 1, in C++. Given a pair of reference image and query template, the pre-processing program marks regions and patches that may match the template and passes the results to a second stage template matching algorithm to pinpoint the exact location of the best match. Three conventional high-precision template matching techniques, SIFT [15], BBS [4] and FAsT-Match [11], are tested as the second stage matching algorithm to demonstrate the effectiveness of the proposed pre-processor for different types of template matching techniques. The implementations of the three tested techniques are from their original authors and executed with the default settings. All of the reported experiments in this paper are carried on a computer with an Intel i7-4770 (3.4GHz) CPU and 8GB memory.

6.1 Exp. I: Image Matching

In this group of experiments, we evaluate the performance of the proposed pre-processing algorithm for high resolution images. The test images come from the MIT database [22], which covers various scenes like urban streets, indoor and natural environments. We select all the 2250 grayscale images in the database with a resolution no less than 640×480 and divide them into three data sets of dif-

Data set	Image size	Template size	Average overlap	Pruning patch	Pruning region	time (s)
I1; T1	640×480	32×32	99.53%	99.71%	81.36%	0.1
I1; T2	640×480	64×64	99.82%	99.72%	74.96%	0.1
I2; T1	960×720	32×32	99.28%	99.79%	88.87%	0.2
I2; T2	960×720	64×64	99.95%	99.84%	81.74%	0.2
I2; T3	960×720	96×96	99.92%	99.88%	74.29%	0.2
I3; T1	1280×960	32×32	99.94%	99.76%	85.87%	0.4
I3; T2	1280×960	64×64	99.98%	99.75%	80.83%	0.4
I3; T3	1280×960	96×96	99.99%	99.74%	77.64%	0.4
I3; T4	1280×960	128×128	99.97%	99.55%	72.63%	0.4

Table 1: Statistical results of each data set for image matching.

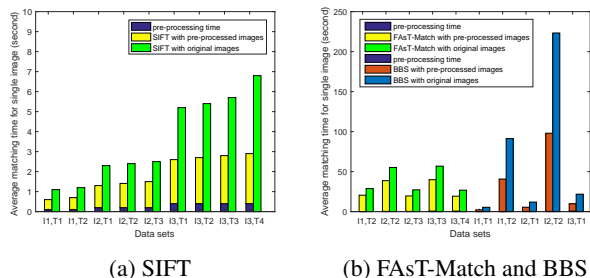


Figure 9: Comparison of the matching times with or without the proposed pre-processing algorithm.

ferent sizes with each set containing 750 images. For each image, we extract 2 templates at random locations with random rotations and then scale them to a given size. The scale range is $[0.5, 2]$, i.e., the scale parameter α, β in Algorithm 1 are 0.5, 2, respectively. To guarantee that these templates can be matched by the conventional template matching techniques in the second stage, we require the standard deviation of the pixel intensities of each template to be above a threshold [19]. As shown in Table 1, 9 different combinations of image and template sizes are used in our experiment. Thus, there are 13500 test cases ($9 \text{ data sets} \times 750 \text{ images} \times 2 \text{ templates}$) in total in this experiment.

With regard to successful screening, we employ a similar definition as in [11]: the regions preserved by the pre-processing algorithm must overlap at least 90% of the area of the ground truth, otherwise, the screening is considered as failed. By this definition, our proposed scheme never fails in any of the 13500 test cases, and on average, more than 99.8% of the ground truth is preserved after the screening, as presented in Table 1. Since the matched patch reported by a conventional template matching algorithm overlaps with the ground truth only by 80% on average in general, our scheme has negligible impact on the accuracy of the second stage algorithm.

Furthermore, our scheme prunes around 80% of the regions on average; and only less than 0.5% of all the candidate patches are marked as possible matches and sent to the second stage algorithm. As a result, the second stage

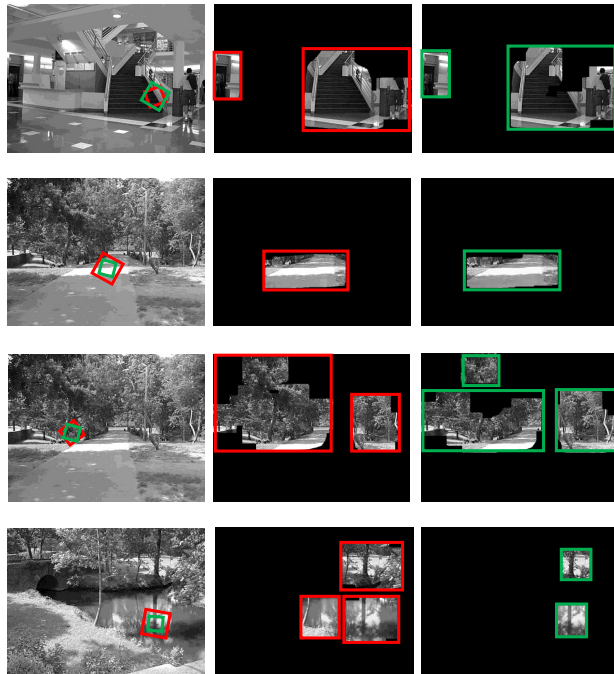


Figure 10: Example of screening results for image matching.

algorithm has much a smaller matching problem to solve and hence requires shorter time. For example, as shown in Figure 9, SIFT uses 50% less time by employing the pre-processing algorithm and FAsT-Match and BBS also have 30% and 55% reductions, respectively, in time on average. We also test BBS with this data set, however, BBS cannot handle the large rotation and scaling properly in the synthetic experiment, failing almost all the test cases. Figure 10 shows some example results using the MIT database. The images in the left column are the reference images with two query templates marked in boxes for each image. The remaining regions after screening are shown in the middle and right columns. In general, the more distinct the template is, the more searching space can be ruled out by the proposed algorithm.

We also use the data set provided in [11, 17], to test our algorithm for images with distortions, like blur, brightness change, viewpoint change, JPEG compression. Using the 90% overlap criterion, our screening algorithm successfully preserves the ground truth in all the cases with blur, zoom, rotation and JPEG compression deformations. But the success ratio falls to around 60% for test cases with significant viewpoint or brightness change. However, overall the screening has negligible impact to the results of the conventional algorithms, as they usually cannot find the best match as well for those difficult cases. As demonstrated in Figure 11 are some sample results for images with different distortions, where the green boxes in the left column mark the templates and the green, red, blue boxes in the mid-

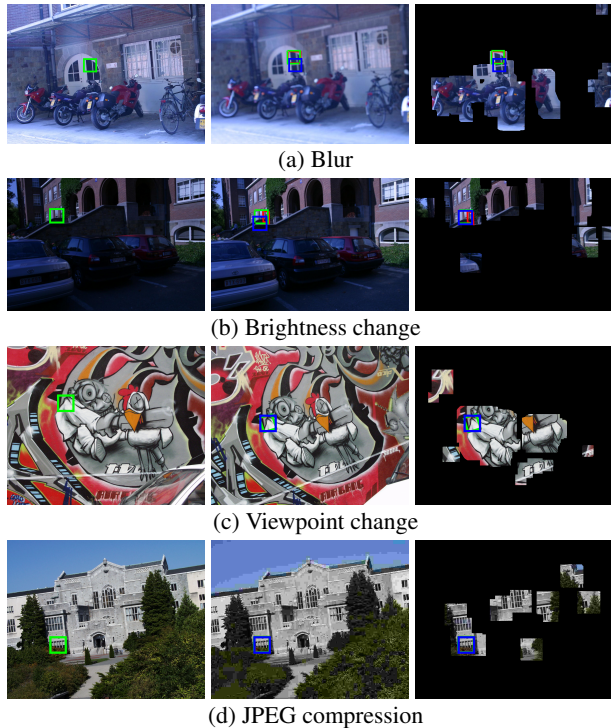


Figure 11: Example of screening results for images with distortions.

Algorithms	Results	Without screening	With screening
FAsT-Match	Time per image (s)	36.2s	25.3s
	Average overlap	41%	41%
	Success ratio	45/105	46/105
BBS	Time per image (s)	16.7s	9.4s
	Average overlap	62%	61%
	Success ratio	75/105	75/105
SIFT	Time per image (s)	1.8s	1.4s
	Average overlap	N/A	N/A
	Success ratio	10/105	10/105

Table 2: Statistical results of each tested algorithm for video tracking.

middle and right columns mark the ground truth, the results by FAsT-Match and the results by BBS, respectively.

6.2 Exp. II: Video Tracking

This group of experiments evaluates our algorithm for video tracking applications. The test set is generated from 35 color video clips provided in the Visual Tracker Benchmark [27]. From each video, we randomly pick three pairs of frames that are 20 frames apart and use the annotated object in the first frame as template and the second frame as reference image for each frame pair. This test set is quite challenging, because the objects of interest typically undergo some non-rigid deformations and may also be partially occluded after 20 frames.

The average running time of our pre-processing algo-

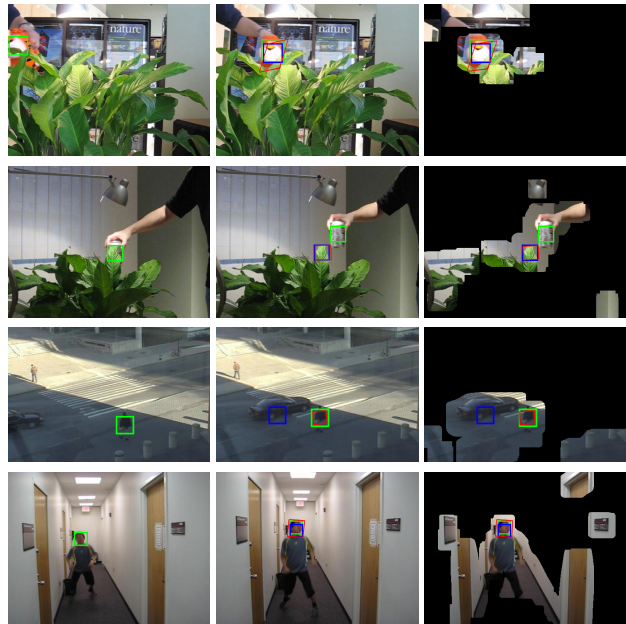


Figure 12: Example of screening results for video tracking.

rithm on this data set is only 0.05s, as the resolution of the videos is relatively low (480×320). On average, our algorithm prunes 88% of the patches and 55% of the regions, and in 95 out of the 105 cases, it preserves more than 90% of the ground truth after screening. Although in some cases, the screening is not successful ($>90\%$ overlap), our proposed algorithm does not adversely affect the success ratio of the tested conventional algorithm at all as shown in Table 2. Interestingly, the success ratio becomes slightly higher for FAsT-Match when the screening algorithm is applied. This is because a conventional algorithm may match to a wrong patch in some cases, but the wrong patch can be recognized and removed by our algorithm beforehand. Some sample results of the video tracking data set are shown in Figure 12. The results of each algorithm are marked in the same way as Figure 11.

7 Conclusion

This paper presents a generic template matching pre-processor for expediting conventional template matching techniques. The proposed pre-processing algorithm can handle arbitrary rotation and scaling of reference images effectively as demonstrated by extensive experiments.

References

- [1] L. G. Brown. A survey of image registration techniques. *ACM computing surveys (CSUR)*, 24(4):325–376, 1992. 2
- [2] M.-S. Choi and W.-Y. Kim. A novel two stage template matching method for rotation and illumination invariance. *Pattern recognition*, 35(1):119–129, 2002. 2

- [3] F. C. Crow. Summed-area tables for texture mapping. *ACM SIGGRAPH computer graphics*, 18(3):207–212, 1984. 2
- [4] T. Dekel, S. Oron, M. Rubinstein, S. Avidan, and W. T. Freeman. Best-buddies similarity for robust template matching. In *Proceedings of the IEEE Conference on Computer Vision and Pattern Recognition*, pages 2021–2029, 2015. 2, 6
- [5] C.-A. Deledalle, J. Salmon, A. S. Dalalyan, et al. Image denoising with patch based pca: local versus global. In *BMVC*, volume 81, pages 425–455, 2011. 3
- [6] M. A. Fischler and R. C. Bolles. Random sample consensus: a paradigm for model fitting with applications to image analysis and automated cartography. *Communications of the ACM*, 24(6):381–395, 1981. 2
- [7] M. Gharavi-Alkhansari. A fast globally optimal algorithm for template matching using low-resolution pruning. *IEEE Transactions on Image Processing*, 10(4):526–533, 2001. 2
- [8] S. Hinterstoisser, C. Cagniart, S. Ilic, P. Sturm, N. Navab, P. Fua, and V. Lepetit. Gradient response maps for real-time detection of textureless objects. *IEEE Transactions on Pattern Analysis and Machine Intelligence*, 34(5):876–888, 2012. 5
- [9] H. Kekre and S. Gharge. Image segmentation using extended edge operator for mammographic images. *International journal on computer science and Engineering*, 2(4):1086–1091, 2010. 3
- [10] H. Y. Kim. Rotation-discriminating template matching based on fourier coefficients of radial projections with robustness to scaling and partial occlusion. *Pattern Recognition*, 43(3):859–872, 2010. 2
- [11] S. Korman, D. Reichman, G. Tsur, and S. Avidan. Fast-match: Fast affine template matching. In *Proceedings of the IEEE Conference on Computer Vision and Pattern Recognition*, pages 2331–2338, 2013. 2, 6, 7
- [12] J. Lewis. Fast normalized cross-correlation. In *Vision interface*, volume 10, pages 120–123, 1995. 2
- [13] R. Lienhart and J. Maydt. An extended set of haar-like features for rapid object detection. In *Image Processing. 2002. Proceedings. 2002 International Conference on*, volume 1, pages I–900. IEEE, 2002. 5
- [14] Y.-H. Lin and C.-H. Chen. Template matching using the parametric template vector with translation, rotation and scale invariance. *Pattern Recognition*, 41(7):2413–2421, 2008. 2
- [15] D. G. Lowe. Distinctive image features from scale-invariant keypoints. *International journal of computer vision*, 60(2):91–110, 2004. 2, 6
- [16] C. Messom and A. Barczak. Fast and efficient rotated haar-like features using rotated integral images. In *Australian Conference on Robotics and Automation*, pages 1–6, 2006. 5
- [17] K. Mikolajczyk and C. Schmid. A performance evaluation of local descriptors. *IEEE transactions on pattern analysis and machine intelligence*, 27(10):1615–1630, 2005. 7
- [18] J.-M. Morel and G. Yu. Asift: A new framework for fully affine invariant image comparison. *SIAM Journal on Imaging Sciences*, 2(2):438–469, 2009. 2
- [19] W. Ouyang, F. Tombari, S. Mattoccia, L. Di Stefano, and W.-K. Cham. Performance evaluation of full search equivalent pattern matching algorithms. *IEEE transactions on pattern analysis and machine intelligence*, 34(1):127–143, 2012. 2, 7
- [20] O. Pele and M. Werman. Accelerating pattern matching or how much can you slide? In *Asian Conference on Computer Vision*, pages 435–446. Springer, 2007. 2
- [21] J. Storer. *An Introduction to Data Structures and Algorithms*. Springer Science & Business Media, 2001. 6
- [22] A. Torralba, K. Murphy, and W. Freeman. The mit csail database of objects and scenes, 2009. 6
- [23] D.-M. Tsai and C.-H. Chiang. Rotation-invariant pattern matching using wavelet decomposition. *Pattern Recognition Letters*, 23(1):191–201, 2002. 2
- [24] F. Ullah and S. Kaneko. Using orientation codes for rotation-invariant template matching. *Pattern recognition*, 37(2):201–209, 2004. 2
- [25] P. Viola and M. J. Jones. Robust real-time face detection. *International journal of computer vision*, 57(2):137–154, 2004. 2
- [26] T. Wakahara and Y. Yamashita. Gpt correlation for 2d projection transformation invariant template matching. In *Pattern Recognition (ICPR), 2014 22nd International Conference on*, pages 3810–3815. IEEE, 2014. 2
- [27] Y. Wu, J. Lim, and M.-H. Yang. Online object tracking: A benchmark. In *Proceedings of the IEEE conference on computer vision and pattern recognition*, pages 2411–2418, 2013. 8